

Comparing plasmonic and dielectric gratings for absorption enhancement in thin-film organic solar cells

Khai Q. Le,^{1,2,*} Aimi Abass,³ Bjorn Maes,^{2,4} Peter Bienstman,² and Andrea Alù¹

¹Department of Electrical and Computer Engineering, The University of Texas at Austin, Austin, Texas 78712, USA

²Photonics Research Group, Department of Information Technology, Ghent University-IMEC, St-Pietersnieuwstraat 41, B-9000 Ghent, Belgium

³Solar Cells Group, Department of Electronics and Information Systems, Ghent University, St-Pietersnieuwstraat 41, B-9000 Ghent, Belgium

⁴Micro- and Nanophotonic Materials Group, Faculty of Science, University of Mons, B-7000 Mons, Belgium
[*khai.le@mail.utexas.edu](mailto:khai.le@mail.utexas.edu)

Abstract: We theoretically investigate and compare the influence of square silver gratings and one-dimensional photonic crystal (1D PC) based nanostructures on the light absorption of organic solar cells with a thin active layer. We show that, by integrating the grating inside the active layer, excited localized surface plasmon modes may cause strong field enhancement at the interface between the grating and the active layer, which results in broadband absorption enhancement of up to 23.4%. Apart from using silver gratings, we show that patterning a 1D PC on top of the device may also result in a comparable broadband absorption enhancement of 18.9%. The enhancement is due to light scattering of the 1D PC, coupling the incoming light into 1D PC Bloch and surface plasmon resonance modes.

©2011 Optical Society of America

OCIS codes: (350.6050) Solar energy; (240.6680) Surface plasmons; (040.5350) Photovoltaic; (250.5403) Plasmonics; (050.2770) Gratings.

References and links

1. H. Hoppe and N. S. Sariciftci, "Organic solar cells: an overview," *J. Mater. Mater. Res.* **19**(07), 1924–1945 (2004).
2. M. Agrawal and P. Peumans, "Broadband optical absorption enhancement through coherent light trapping in thin-film photovoltaic cells," *Opt. Express* **16**(8), 5385–5396 (2008).
3. S. H. Park, A. Roy, S. Beaupre, S. Cho, N. Coates, J. S. Moon, D. Moses, M. Leclerc, K. Lee, and A. J. Heeger, "Bulk heterojunction solar cells with internal quantum efficiency approaching 100%," *Nat. Photonics* **3**(5), 297–302 (2009).
4. G. F. Burkhard, E. T. Hoke, S. R. Scully, and M. D. McGehee, "Incomplete exciton harvesting from fullerenes in bulk heterojunction solar cells," *Nano Lett.* **9**(12), 4037–4041 (2009).
5. T. Soga, *Nanostructured Materials for Solar Energy Conversion*, (Elsevier Science, Amsterdam, 2006).
6. H. A. Atwater and A. Polman, "Plasmonics for improved photovoltaic devices," *Nat. Mater.* **9**(3), 205–213 (2010).
7. G. E. Jonsson, H. Fredriksson, R. Sellappan, and D. Chakarov, "Nanostructures for enhanced light absorption in solar energy devices," *Int. J. Photoenergy* **2011**, 939807 (2011).
8. S. S. Kim, S. I. Na, J. Jo, D. Y. Kim, and Y. C. Nah, "Plasmon enhanced performance of organic solar cells using electrodeposited Ag nanoparticles," *Appl. Phys. Lett.* **93**(7), 073307 (2008).
9. Y. A. Akimov, W. S. Koh, and K. Ostrikov, "Enhancement of optical absorption in thin-film solar cells through the excitation of higher-order nanoparticle plasmon modes," *Opt. Express* **17**(12), 10195–10205 (2009).
10. H. Shen, P. Bienstman, and B. Maes, "Plasmonic absorption enhancement in organic solar cells with thin active layers," *J. Appl. Phys.* **106**(7), 073109 (2009).
11. A. Abass, H. Shen, P. Bienstman, and B. Maes, "Angle insensitive enhancement of organic solar cells using metallic gratings," *J. Appl. Phys.* **109**(2), 023111 (2011).
12. C. Min, J. Li, G. Veronis, J. Y. Lee, S. Fan, and P. Peumans, "Enhancement of optical absorption in thin-film organic solar cells through the excitation of plasmonic modes in metallic gratings," *Appl. Phys. Lett.* **96**(13), 133302 (2010).
13. R. A. Pala, J. White, E. Barnard, J. Liu, and M. L. Brongersma, "Design of plasmonic thin-film solar cells with broadband absorption enhancements," *Adv. Mater. (Deerfield Beach Fla.)* **21**(34), 3504–3509 (2009).

14. C. Heine and R. H. Morf, "Submicrometer gratings for solar energy applications," *Appl. Opt.* **34**(14), 2476–2482 (1995).
 15. M. Niggemann, M. Glatthaar, A. Gombert, A. Hinsch, and V. Wittwer, "Diffraction gratings and buried nano-electrodes-architectures for organic solar cells," *Thin Solid Films* **451–452**, 619–623 (2004).
 16. M. Kroll, S. Fahr, C. Helgert, C. Rockstuhl, F. Lederer, and T. Pertsch, "Employing dielectric diffractive structures in solar cells - a numerical study," *Phys. Status Solidi A* **205**(12), 2777–2795 (2008).
 17. G. F. Burkhard, E. T. Hoke, and M. D. McGehee, "Accounting for interference, scattering, and electrode absorption to make accurate internal quantum efficiency measurements in organic and other thin solar cells," *Adv. Mater. (Deerfield Beach Fla.)* **22**(30), 3293–3297 (2010).
 18. Y. Park, E. Drouard, O. El Daif, X. Letartre, P. Viktorovitch, A. Fave, A. Kaminski, M. Lemitte, and C. Seassal, "Absorption enhancement using photonic crystals for silicon thin film solar cells," *Opt. Express* **17**(16), 14312–14321 (2009).
 19. O. El Daif, E. Drouard, G. Gomard, A. Kaminski, A. Fave, M. Lemitte, S. Ahn, S. Kim, P. Roca I Cabarrocas, H. Jeon, and C. Seassal, "Absorbing one-dimensional planar photonic crystal for amorphous silicon solar cell," *Opt. Express* **18**(S3), A293–A299 (2010).
 20. P. Bermel, C. Luo, L. Zeng, L. C. Kimerling, and J. D. Joannopoulos, "Improving thin-film crystalline silicon solar cell efficiencies with photonic crystals," *Opt. Express* **15**(25), 16986–17000 (2007).
 21. D. Duché, E. Drouard, J. J. Simon, L. Escoubas, P. Torchio, J. Le Rouzo, and S. Vedraïne, "Light harvesting in organic solar cells," *Sol. Energy Mater. Sol. Cells* **95**, S18–S25 (2011).
 22. COMSOL, www.comsol.com
-

1. Introduction

Thin-film organic solar cells (OSCs) have attracted intensive research interest due to their potential for low-cost photovoltaic devices [1]. However, the development of these devices is hampered by their low efficiency, since the active layer thickness must be smaller than the exciton diffusion length [2], which causes a limited photon absorption rate. To overcome the diffusion length problem, the concept of bulk heterojunction (BHJ) was introduced [3]. However, even with a BHJ the thickness is still restricted to thin films on the order of 200 nm for optimal electronic properties [4]. Above these thicknesses, the energy conversion efficiency drops since free-carrier recombination becomes significant [5].

Several techniques have been introduced to improve the optical absorption of OSCs [6,7]. Many involve the use of metallic nanostructures which causes the excitation of surface plasmon modes. These modes can offer several ways to enhance the absorption, while reducing the bulk volume and the thickness of the active layer. One of those is resonant scattering caused by the scattering of the incoming light on metallic nanoparticles. It leads to light coupled and trapped into the absorbing layer [8]. Apart from using metallic nanoparticles as scatterers, they are used as optical antennas to convert incident light into localized surface plasmon modes, which result in a strong field enhancement around the particle or a near-field enhancement due to plasmonic near-field coupling between particles to enhance absorption efficiency [9,10]. In addition, introducing periodic structures has been shown to be a very promising way to efficiently trap light and enhance absorption efficiency [11–16]. Enabling the coupling of sunlight to plasmonic guided modes and/or exciting localized surface plasmon modes can be done, for example, by simply engineering the metallic back contact, which has been demonstrated to be an effective way to boost the optical absorption [11]. Recently, much attention has been given to the usage of plasmonic gratings embedded on top of the active layer [12,13]. Min et al. [12] proposed a design in which the grating structure is embedded in the transparent electrode with a very thin active layer of around 15 nm, which may cause big challenges in fabrication, but could lead to a large exciton collection efficiency. Currently, the thinnest thin-film OSCs that have been successfully fabricated are around 48–60 nm active layer thickness [17]. Their absorption rate, however, is still quite limited.

In this work, we employ a silver (Ag) periodic grating placed inside the active layer to improve the optical absorption of a thin organic photovoltaic cell (60 nm active layer thickness). Silver is chosen since it allows for low metal absorption loss and it also has a beneficial surface plasmon resonance wavelength suitable for enhancing a P3HT:PCBM organic solar cell. With the grating integrated inside the active layer a strong field enhancement was observed for surface plasmon modes excited at the interface between the

grating and the active layer. In addition, there is a resonant near field enhancement due to the excitation of propagating surface plasmon modes on the metal back contact enabled via coupling between the localized surface plasmon mode of the grating and surface plasmon mode of the metal back contact. These coupled plasmon modes contribute to broadband absorption enhancement in the active layer.

Apart from using plasmonic nanostructures to enhance the performance of thin-film solar cells, patterning 1D or 2D PC on the cell may also improve their absorption efficiency. Recent advances in using these PC based structures for enhanced absorption have been reported in thin-film solar cells [18–21]. However, directly having the active solar material in a PC structure as proposed by these groups may lead to electronic problems, as it would mean more free surfaces which can act as charge carrier traps. In this work, we consider using a 1D PC on top of a photovoltaic cell, instead of directly inside the active layer, and compare it with a conventional plasmonic grating structure. It is interesting to see how far the absorption enhancement given by dielectric structures can compete with plasmonic structures for enhanced near-field enhancement. This enhancement indeed leads to increased absorption, but it also implies that a major part of the absorption is occurring close to the metal surface, which makes the generated charge carriers more susceptible to many loss mechanisms associated with the metal and does not necessarily translate into conversion to electric energy.

In Section 2, we will describe a solar cell structure and modeling method. In section 3, an absorption enhancement in thin-film organic solar cells by plasmonic and dielectric gratings is presented followed by conclusions in Section 4.

2. Solar cell structure and modeling method

The sketch of the reference device structure is depicted in Fig. 1. The transparent anode is made by 120 nm thick indium tin oxide (ITO) and deposited on a 40 nm thick highly conductive hole transport layer, poly (3, 4-ethylenedioxythiophene): poly (styrenesulfonate) (PEDOT:PSS). The latter is a polymer with good thermal and chemical stability, and good flexibility. The commonly used active layer BHJ material consists of the electron donor poly(3-hexylthiophene) (P3HT) and the electron acceptor (6,6)-phenyl-C61-butyric-acid-methyl ester (PCBM). Results for 60 nm thick polymer layer (P3HT:PCBM) with 1:1 weight ratio are presented here, in contact with the cathode made of silver (Ag). All material properties can be found in [10,11].

There are many numerical techniques that have been successfully employed to calculate the light absorption of the active layer of solar cells, including finite-difference time-domain (FDTD) methods, finite-element methods (FEM), the transfer matrix model (TMM) and the rigorous coupled wave analysis (RCWA). In this work, the calculation of light absorption is carried out by two-dimensional (2D) FEM, as implemented in the COMSOL Multiphysics software package [22]. We assume the light illumination on the device as incident plane waves under TM polarization with wavelengths of 300-800 nm which is the region of interest for the P3HT:PCBM material. Periodic boundary conditions are set at the left and right boundaries, while perfectly matched layer (PML) absorbing boundary conditions are used at the top and bottom boundaries of the computational domain. The absorption in the active layer is calculated by integrating the divergence of the Poynting vector (power flow) which is then normalized with input power.

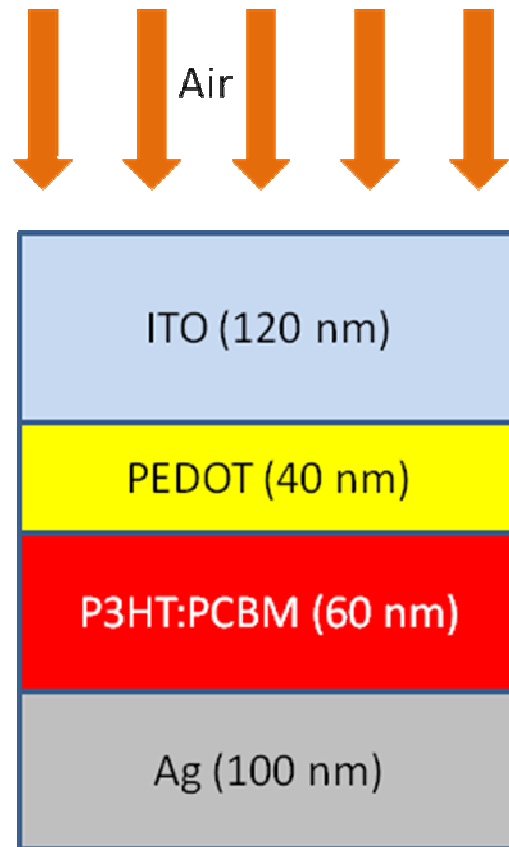


Fig. 1. Cross-section of the reference flat OSC.

3. Results and discussions

3.1 Enhanced absorption by square Ag gratings

It has been demonstrated that the use of metallic gratings on top of the solar cell (on top of the contacts), or integrated inside the PEDOT electrode, or even partially in the active layer (half the grating inside the active layer and half in the PEDOT electrode), can result in optical field enhancement, and can lead to larger optical absorption.

Putting gratings on top of solar cell can result in high scattering of light and trap light effectively in the active layer in the wavelength range 400-600 nm. Efficient scattering from the top surface, however, requires larger structures, which are not easily integrated in organic device structures. Integrating gratings in PEDOT and partially inside the active layer can generate the excitation of localized surface plasmon resonances (LSPRs) to obtain near-field enhancement and result in enhanced light absorption. In this work, we propose to integrate optical gratings more inside the active layer. Apart from just offering strong light scattering and effective light trapping in the active layer, near field enhancement by the plasmonic structure is utilized to the fullest when the metal is embedded in the active material and we show effective excitation of LSPR modes at the interface between the grating and the active layer. In addition, this results in a resonant near field enhancement due to the excitation of propagating surface plasmon modes (SPRs) on the metal back contact enabled via coupling between the LSPR of the grating and SPR of the metal back contact. These coupled plasmon modes contribute to broadband absorption enhancement in the active layer.

The sketch of the proposed device structure is shown in Fig. 2. This can cause the excitation of localized surface plasmon resonance (LSPR) modes at the interface between the grating and the active layer leading to strong field enhancement. In addition, these LSPR modes can couple to SP modes occurring at the interface between the active layer and the Ag back contact, which results in absorption enhancement in the active layer.

Now, we start to look for the optimal dimension W and periodicity P of the grating to ensure highest absorption enhancement. Here, the enhancement factor is defined as

$$\frac{\sum_{\lambda} A_{\text{grating}}(\lambda, W, P) - \sum_{\lambda} A_0(\lambda)}{\sum_{\lambda} A_0(\lambda)}$$

where A_{grating} and A_0 are the absorption in the active layer with and without the grating as a function of wavelength, respectively. Figure 3 depicts the absorption enhancement for various sizes of the square grating and the periodicity. It is found that a maximum enhancement of up to 23.4% is obtained at the optimal size of 46 nm and periodicity of 350 nm. By calculating the absolute absorption of this optimum structure, we found that the active layer absorbs 58.7% of the AM 1.5G spectrum in the wavelength range 300-800 nm.

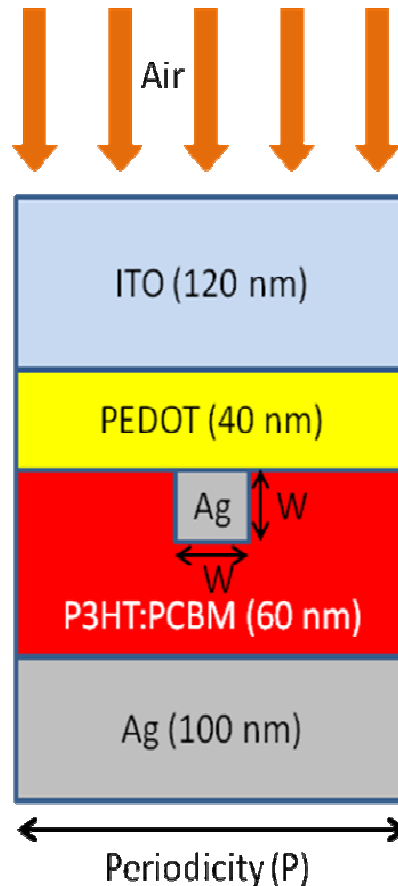


Fig. 2. Cross-section of OSC with Ag square grating integrated inside the active layer.

The absorption spectra of the OSC with this optimal grating and the flat cell are shown in Fig. 4, where a broadband absorption enhancement is observed. The enhancement is due to

the excitation of localized surface plasmon modes at the interface between the Ag grating and the active layer. Figure 5 shows contour plots of the absorption profiles, capped at a certain maximum value for clarity. It is observed that, at the wavelength of 350 nm, light is mostly absorbed by the Ag grating, which causes less absorption than the flat cell. However, this only results in negligible loss, as the solar energy for wavelengths below 350 nm is already limited. In the more relevant range, 410-650 nm, the localized surface plasmon modes excited at the interface between the grating and the active layer cause strong field enhancement around the interface. The field is mainly distributed in the active layer rather than inside the metal as we go to longer wavelengths. This results in an improvement of the absorption efficiency of the active layer, particularly around the edges of the metal grating.

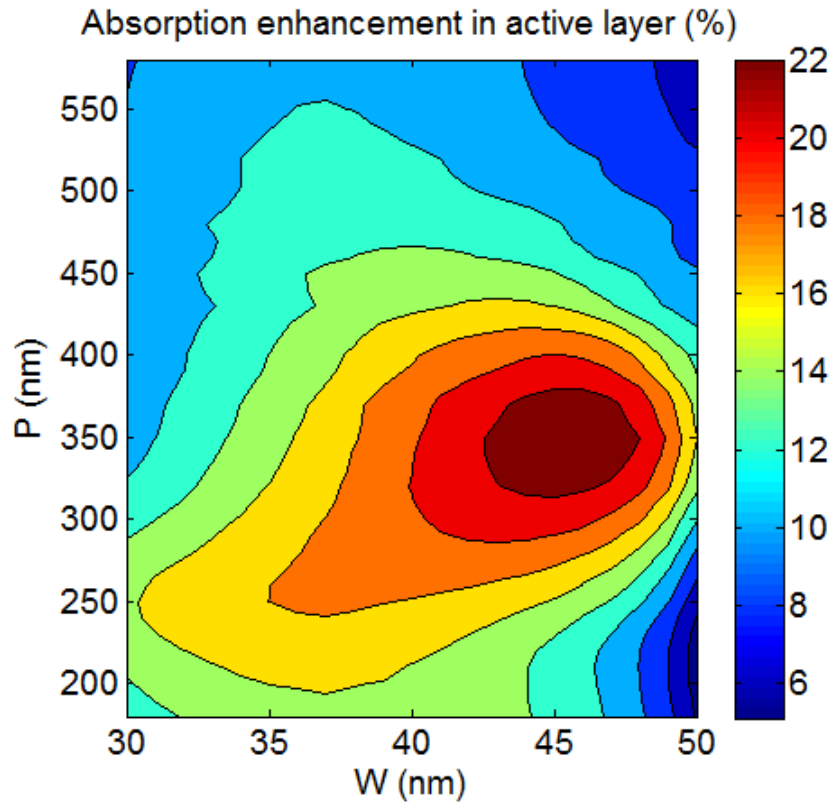


Fig. 3. Absorption enhancement in active layer for various sizes of Ag square grating with width (W) and periodicity (P).

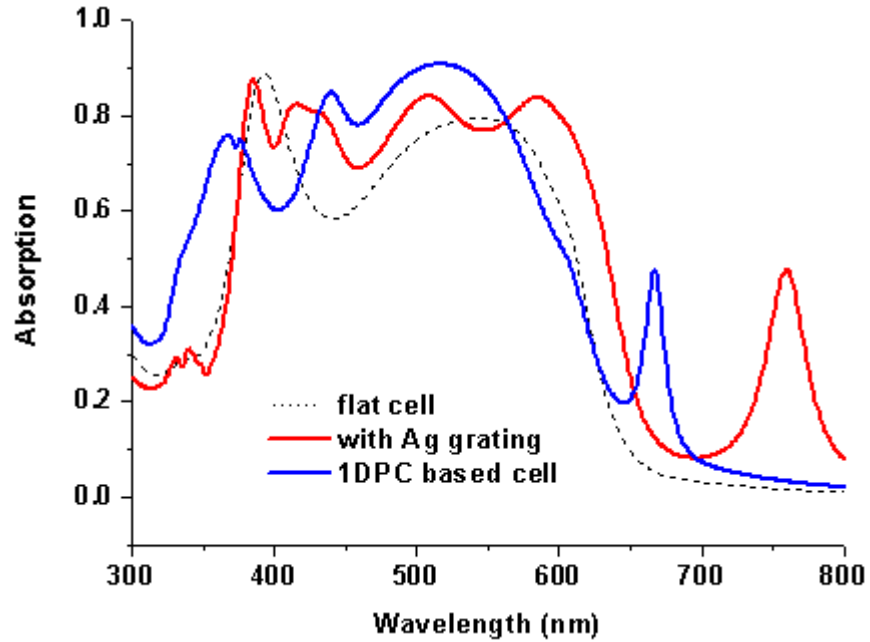


Fig. 4. Absorption in the active layer for the bare OSC (dotted line), the cell with Ag square grating (red solid line), and 1D PC (blue solid line).

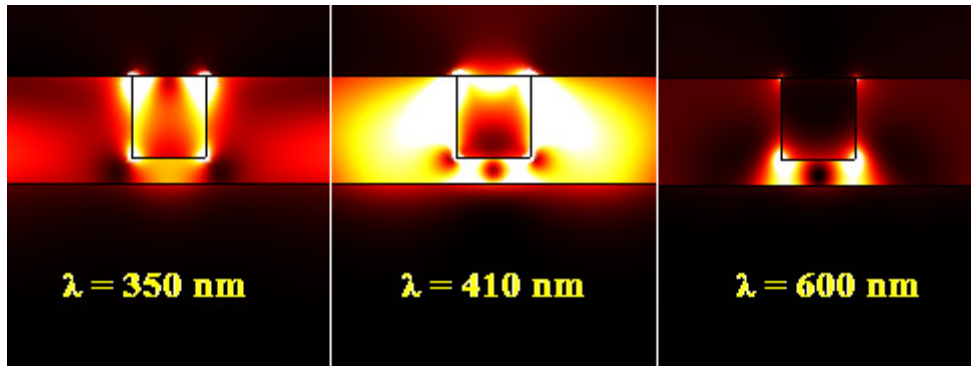


Fig. 5. Absorption profiles of OSCs with optimal Ag square grating with $W = 46$ nm and $P = 350$ nm at various wavelengths (λ).

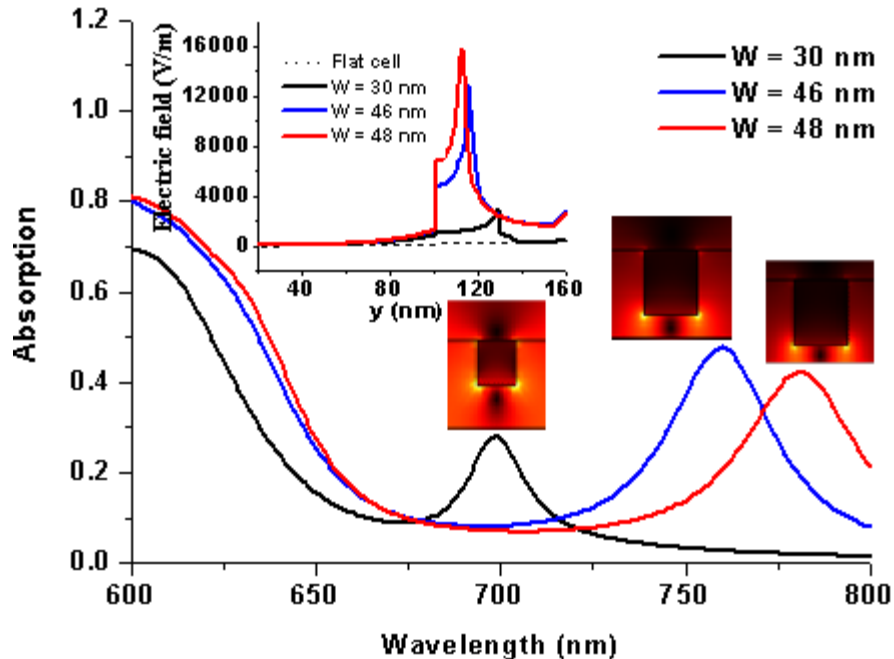


Fig. 6. Absorption in active layer for various sizes of Ag square grating (the absorption profiles corresponding to the absorption peaks are shown above the peaks). The inset is a cross-section of the field along the edge of the grating, from air to the active layer side.

Furthermore, Fig. 4 shows a peak in the absorption spectrum at $\lambda = 750$ nm. This absorption resonance is sensitive to the distance between the grating and the Ag back contact (see Fig. 6). Upon investigating the field pattern at these peaks for various sizes of the grating (Fig. 6), we see that the SPR mode is excited at the interface between the active layer and the Ag back contact. This mode is coupled to the LSPR mode of the grating resulting in a strong near-field enhancement. The inset of Fig. 6 shows electric field curves along the edge of the optimal grating ($W = 46$ nm, $P = 350$ nm). A very strong enhancement compared to the flat cell is observed around the corner of the grating. In addition, from Fig. 6 we can see that when W increases, the resonance wavelength redshifts. Unsurprisingly, smaller grating-electrode distances lead to larger field enhancements. However, the resulting absorption peak is shifted far away from the wavelength region of interest as the distance decreases. Therefore a trade-off is observed, and the optimal width is $W = 48$ nm. Gratings with $W \geq 48$ nm have stronger near-field enhancements but the resonance peak is shifted far away from the wavelength of interest.

3.2. Enhanced absorption by 1D PC based structures

Besides using metallic nanostructures integrated in the device to boost the absorption, patterning 1D or 2D PCs on the solar cell may also result in absorption enhancement in thin-film solar cells [18–21]. In this case, the incident light can be coupled into Bloch modes of the PC, with increased photon travelling time in the active material. In this section, we simulate a 1D PC pattern of the ITO and PEDOT layers, see Fig. 7, and investigate how it affects the absorption of the OSC. In this case, special care is needed in designing the PC to enable light coupling into Bloch modes in the desirable wavelength region. The geometrical parameters of the PC should be scanned to find an optimal configuration.

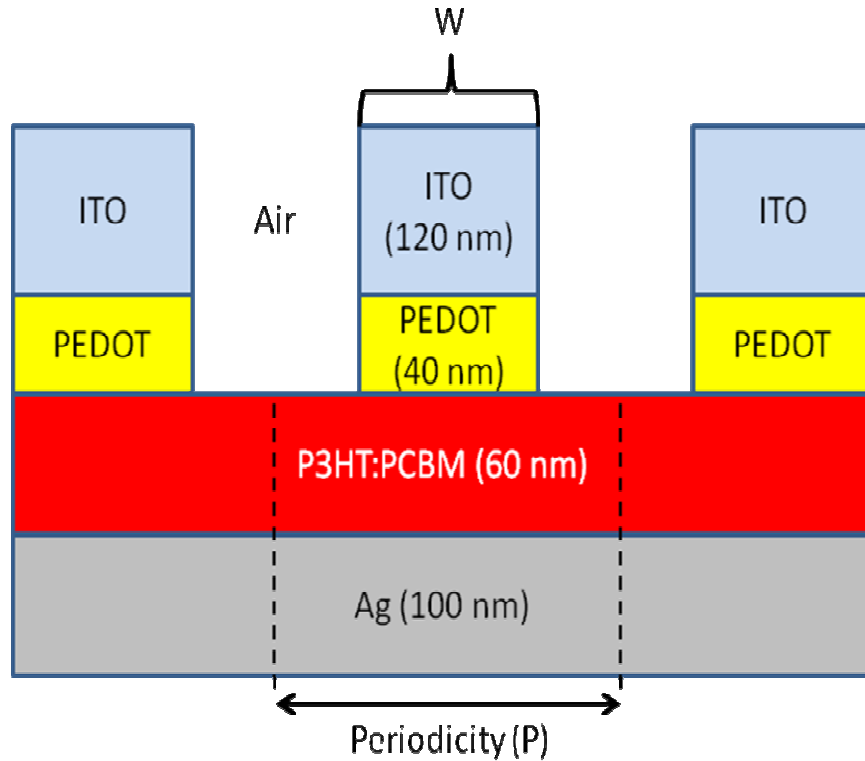


Fig. 7. Cross-section of OSC with 1D photonic crystal patterned on top.

Using the same definition of enhancement factor, we find the optimal structure defined by W (width of ITO and PEDOT) and P (periodicity), as shown in Fig. 8. The maximum enhancement factor with this structure is limited to 18.9% corresponding to the optimal $W = 180$ nm and $P = 375$ nm. The calculated absolute total absorption of the AM 1.5G solar spectrum in the wavelength range 300-800 nm for this dielectric grating structure is around 56.14%.

The absorption spectra of the OSC with this optimal 1D PC and the flat cell are depicted in Fig. 4. Significant broadband absorption enhancement via scattering and interference effects is achieved with the 1D PC structure, similar to the plasmonic geometry considered above. At certain wavelengths, e.g. 370 nm or 520 nm, most of the incoming light is focused into the active layer, as seen in Fig. 9, producing enhanced absorption. Absorption enhancement does not happen for all wavelengths though. For instance, at the wavelength of 400 nm, less absorption is observed since only little part of the incoming light is scattered into the active layer and most of it is reflected back.

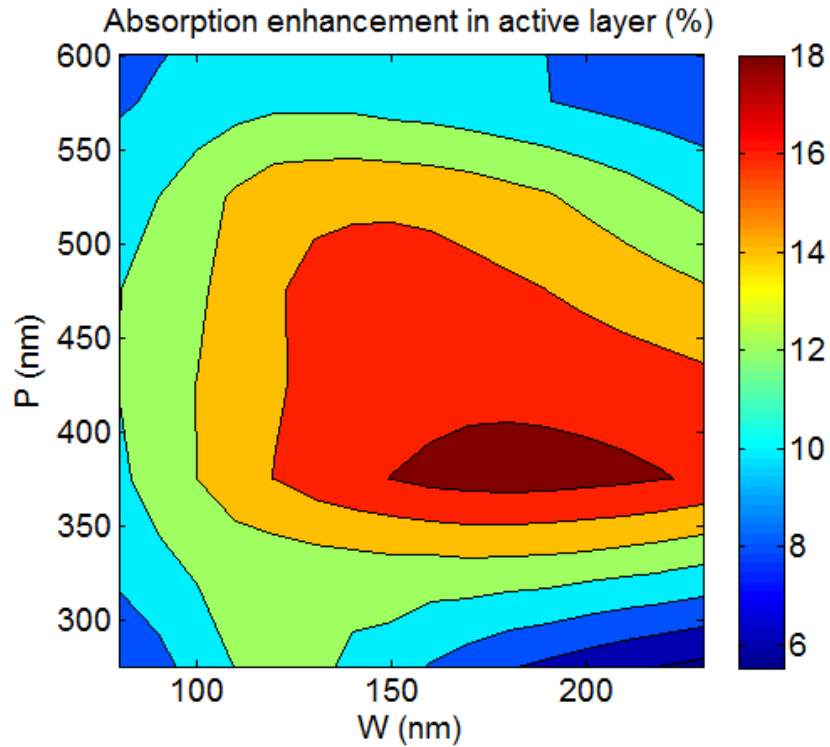


Fig. 8. Absorption enhancement in the active layer varying the ITO width (W) and periodicity (P).

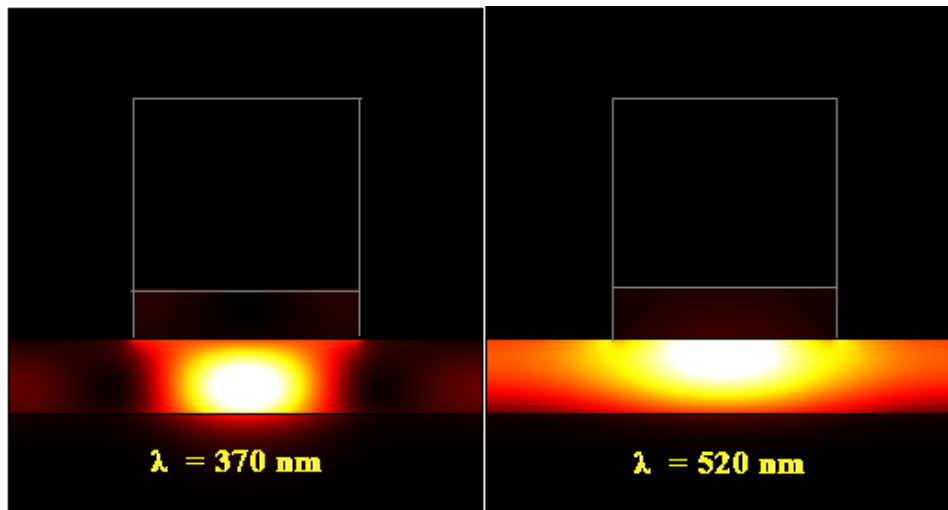


Fig. 9. Absorption profiles of OSC with 1D PC grating at various wavelengths (λ).

This periodic dielectric structure also excites an SPR mode at the interface of the active layer and the Ag back contact at $\lambda = 670$ nm. Examining the field pattern of this mode (Fig. 10), we see strong field enhancement confined close to the metal surface, typical of a surface-plasmon mode. This resonant mode also strongly influences the enhancement factor. The corresponding resonant wavelength is linearly shifted with an increase of periodicity P, as seen in Fig. 11. Care should be paid to make sure that the resonance mode still resides within the wavelength range of interest.

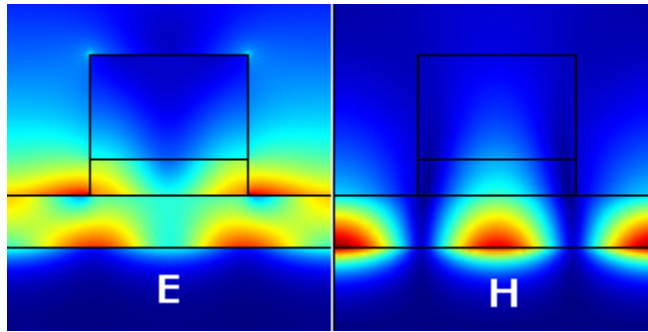


Fig. 10. Electric and magnetic field at SPR mode with $\lambda = 670$ nm.

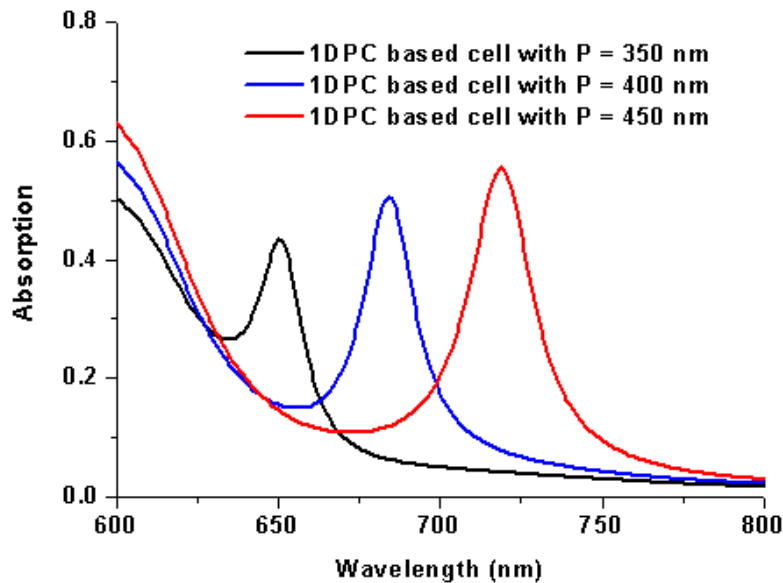


Fig. 11. Absorption in the active layer of a flat cell and of a 180 nm width 1D PC cell, for various periodicities.

Besides enhancement due to light scattering and SPR mode excitation, another resonance peak is observed at 440 nm wavelength. By modal analysis of the structure, we found a Bloch mode at $k = 0$ existing along the plane of the structure at 446 nm, which is close to the peak in the absorption spectrum. The field profile of the mode can be seen in Figs. 12(a) and 12(b), which show the amplitude of the electric and magnetic fields, respectively. Significant absorption enhancement is obtained by exciting this mode, although the field profile is mainly distributed above the active absorbing solar cell layer. Figure 12(c) shows the electric field distribution in the case of excitation at normal incidence at 440 nm wavelength. We see a correspondence between the profiles in Figs. 12(a) and 12(c), indicating that the absorption peak is really due to the excitation of this mode. Further optimization of the field profile to further shift the distribution into the active layer can still be performed by tuning the thickness of the ITO and PEDOT layer. In addition, the field profile significantly extends into the air layer above the structure, which is expected as the mode propagates through air in certain regions of the periodic structure. This could be reduced by filling the gaps with some dielectric substrate.

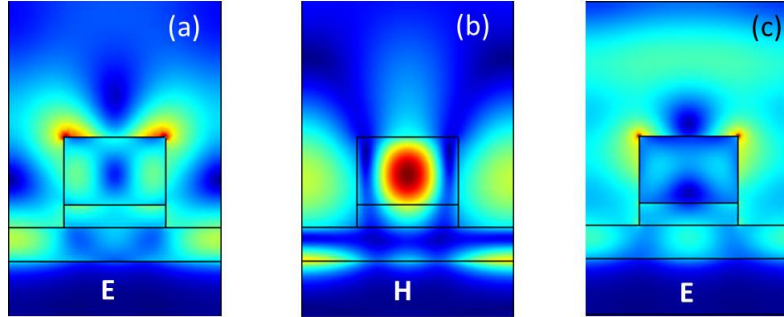


Fig. 12. (a) Electric and (b) magnetic field profiles of a guided Bloch mode at 446 nm. (c) Electric field profile in the case of normal incidence plane wave upon the structure at wavelength $\lambda = 440$ nm.

The use of a periodic dielectric structure may be more advantageous than the plasmonic geometry considered above, as the absorption enhancement is more evenly distributed throughout the active material. In metallic periodic structures the absorption enhancement, especially by LSPRs, tends to be concentrated close to the metal, which increases the possibility that the absorbed photons will not contribute to current generation. This is due to either improper passivation of surface states on the metal interface or other exciton quenching effects which depend on the distance from a metal interface. If the absorption enhancement by the metal structure is large enough, these loss mechanisms may not be so detrimental. We show here, however, the possibility of achieving comparable, although still smaller, absorption enhancement with a periodic dielectric structure. More studies need to be done, but the comparison here indicates that we may not need to rely on metal nanostructures to achieve a good absorption enhancement.

4. Conclusions

We have demonstrated the possibility of achieving absorption enhancement in thin-film OSCs by integrating Ag gratings inside the thin active layer or alternatively patterning the 1D PC on top of the cell. Ag gratings cause the excitation of LSPR modes at the grating surface and the coupling of these modes with SPR modes at the back contact surface. 1D PC based structures achieve enhancement due to scattering and light coupling into Bloch modes, and the excitation of SPR modes at the back contact surface. The realized optimal absorption enhancement in the case of Ag gratings is about 23.4%, and in the case of 1D PC we found about 18.9%. Although the enhancement factor from the 1D PC is smaller than that of the Ag grating, the fabrication of the former structure may be much easier, and still give significant enhancement.

Acknowledgments

This research was supported by the IWT Institute for the Promotion of Innovation by Science and Technology in Flanders via the SBO-project “Polyspec” and “SilaSol”, by the Interuniversity Attraction Poles program of the Belgian Science Policy Office under Grant No. IAP P6-10 “photonics@be”, by COST Action MP0702 and by an NSF CAREER award No. ECCS-0953311.